Violation of Auditory Regularities is Reflected in Pupil Dynamics

Hamit Basgol[1,2,3], Peter Dayan[1,4] and Volker H. Franz[1,2]

[1]Department of Computer Science, University of Tübingen, Tübingen, Germany

[2]Experimental Cognitive Science, University of Tübingen, Tübingen, Germany

[3]The Graduate Training Centre of Neuroscience, University of Tübingen, Tübingen, Germany

[4]Max Planck Institute for Biological Cybernetics, Tübingen, Germany

Author Note

Correspondence concerning this article should be addressed to Hamit Basgol, Experimental Cognitive Science, University of Tübingen, Sand 6, 72074, Tübingen, Germany. Email: hamit.basgoel@uni-tuebingen.de.

Word count: 7313 (excluding references)

Abstract

The brain maintains internal models to make predictions. When predictions are violated, the current model can either be updated or replaced by a new model. The latter is accompanied by pupil dilation responses (PDRs) related to locus coeruleus activity/norepinephrine release (LC-NE). We replicated and generalized Zhao et al. (Nature Communications, 2019) by investigating PDRs associated with transitions between regular and random patterns of tones in auditory sequences. We presented these sequences to participants who had been instructed to find silent gaps (to maintain attention). Transitions from regular to random patterns induced PDRs, suggesting that an internal model attuned to the regular pattern is reset. Transitions from one regular pattern to another regular pattern also induced PDRs with later pupil constriction, suggesting also a model reset. On the other hand, transitions from random patterns to regular patterns did not induce PDRs, suggesting a gradual update of model parameters because the random pattern does not allow for strong predictions. Overall, our results replicate Zhao et al. (2019) closely and suggest that PDRs, a biomarker of LC-NE activation, are indeed sensitive to model reset but not model update.

Keywords: internal model reset, regularity violations, pupil dilation responses, the locus coeruleus norepinephrine system

Word count: 185

1. Violation of Auditory Regularities is Reflected in Pupil Dynamics

The sensory input from natural environments exhibits statistical regularities over multiple temporal and spatial scales. A wide range of studies has observed that humans are sensitive to these statistical regularities and track them (Frost et al., 2019; Barascud et al., 2016; Paavilainen, 2013; Sherman et al., 2020; Zhao et al., 2019; Canale, 2022) to improve their performance in perceptual and cognitive tasks (Bestmann et al., 2008; Krishnamurthy et al., 2017). However, existing statistical regularities in the environment are constantly violated, and new regularities emerge.

In this study, we replicated and generalized the results of Zhao et al. (2019), who observed that the readily detectable violation of such statistical regularities (i.e., deviations from regular patterns) but not their emergence from random patterns led to sharp increases in pupil size (i.e., pupil dilation responses, PDRs in short). They interpreted these PDRs as reflecting the activity of the locus coeruleus-norepinephrine (LC-NE) system, a vital part of the arousal system in the brain. The results were taken as suggesting that an internal model, reflecting a regular pattern, resets upon encountering a random pattern. Conversely, the internal model for a random pattern does not reset but instead undergoes a gradual update in its parameters, as violation of randomness is statistically harder to determine. Hence, the reset of internal models, rather than their update, leads to PDRs.

To investigate whether the discovery of Zhao et al. (2019) was stimulus-specific, we generalized their results using conceptually similar stimuli. In our replication and generalization, we found remarkably similar PDRs with the same magnitude as those observed by Zhao et al. (2019).

1.1 Expected and unexpected uncertainties

Internal models of statistical relationships in the environment are affected by continuous changes and thereby encounter uncertainties (Dayan & Yu, 2003, 2006; Yu & Dayan, 2005; Wilson et al., 2013; Gershman & Niv, 2010). Two types of uncertainties can be defined: expected and unexpected

uncertainties. **Expected uncertainties** arise because of modelled unreliability of predictive relationships and mirror the inherent stochasticity of the environment. When these uncertainties are epistemic rather than aleatoric, they can lead to **model update**. **Unexpected uncertainties** invalidate models, requiring them to be replaced (Dayan & Yu, 2003, 2006; Payzan-LeNestour et al., 2013; Nassar et al., 2012; Yu & Dayan, 2005; Zhao et al., 2019), thus leading to **model reset.**

Expected and unexpected uncertainties suppress top-down expectations and increase the importance of newly acquired information (Dayan & Yu, 2003, 2006; Farashahi et al., 2017; Soltani & Izquierdo, 2019). The difference between expected and unexpected uncertainty is putatively accompanied by differences in the release of neuromodulators, as uncertainties signal when computation and plasticity are required. Thus, environmental changes can drive the brain's arousal systems. Expected uncertainty has been related to the neuromodulator acetylcholine (ACh) and unexpected uncertainty with norepinephrine (NE; Dayan & Yu, 2003; Bouret & Sara, 2005; Marshall et al., 2016; Nassar et al., 2012; Yu & Dayan, 2005).

1.2 The LC-NE system and PDRs

In keeping with this suggestion, one role for the LC-NE system is regulating arousal via widespread NE release (Aston-Jones & Cohen, 2005; Carter et al., 2010; Joshi & Gold, 2020; Nassar et al., 2012; Sara & Bouret, 2012). Indeed, NE has been suggested as the medium by which unexpected uncertainties lead to a global reset signal across the brain (Bouret & Sara, 2005; Dayan & Yu, 2006; Yu & Dayan, 2005; Zhao et al., 2019); this then disrupts top-down cognitive processes and prioritizes the accumulation of bottom-up sensory information, thereby accelerating the discovery and establishment of models of new structure in the environment.

Neurological studies of animal models suggest that PDRs correlate with the LC-NE system's phasic activity (Strauch et al., 2022). For example, Reimer et al. (2016) found that phasic activity in NE

projections was associated with PDRs in mice; Joshi et al. (2016) observed that the activation of the LC-NE system came before an increase in pupil size. Further research based on fMRI (Functional magnetic resonance imaging) suggested that pupil size was positively correlated with BOLD activity in the LC in humans (de Gee et al., 2017; Murphy et al., 2014). Therefore, from this perspective, PDRs can be considered a biomarker of the LC-NE system activity. The relationship of PDRs with arousal and learning rate strengthens this idea further (Nassar et al., 2012).

1.3 Purpose of the Present Study

We examined PDRs to the violation and emergence of regularities in fast-paced auditory sequences. Because we were interested in the automatic processing of statistical regularities, no task was associated with transitions between patterns. Instead, participants were instructed to find gaps in those patterns to ensure that they maintained their attention to the auditory sequences. All this —as well as the bulk of the rest of our experimental design— is analogous to Zhao et al. (2019).

Figure 1A describes typical patterns we used. For each pattern, we also applied the variable-order Markov model IDYOM (information dynamics of music; Pearce, 2005) to estimate the computational requirements for detecting transitions between patterns. The results of this analysis are shown in Figure 1B.

The two most basic patterns are the REG10 and RAND10 patterns. To create these, we first drew 10 tones randomly (with replacement) from a pool of 20 frequencies. For REG10, we presented those 10 tones repeatedly in a fixed order. For RAND10, we presented those 10 tones repeatedly but shuffled them before each presentation. These two conditions were used as baselines because they did not involve a change of their statistical structure. Next, we introduced changes of the statistical structure in three different ways:

Figure 1

Example stimuli and information content values

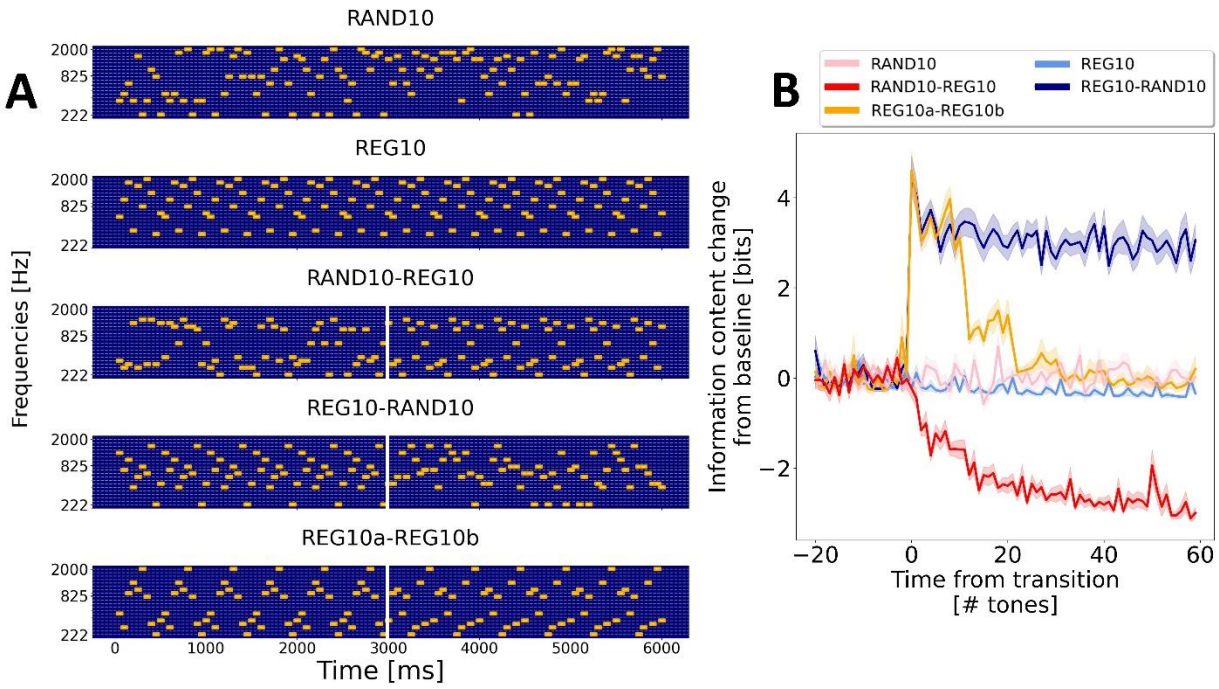

Note. (A) An example set of stimuli used in the experiment. Each tone lasts 50 ms. A white vertical line marks transitions between auditory patterns where they occur (transitions were jittered in the experiment but shown as overlapping for visualization). (B) The average baseline corrected information content values calculated by IDYOM for all trials that one of the participants observed during the experiment. Zero represents transition times to the following pattern. For RAND10-REG10, transition times are shifted one cycle (10 tones, 500 ms), given that the first ten tones in REG10 are indistinguishable from random sequences of tones. For baseline correction, the mean of the 1-second interval before the transition (tones from -20 to 0) was computed and subtracted from each trial. The shaded area represents the standard error of the mean (SEM).

(a) In RAND10-REG10, we used transitions between random and regular patterns of tones. It is known that the transition from a random to a regular pattern evokes a transient increase in the MEG (Magnetoencephalography) response (Barascud et al., 2016). This transient increase is associated with the predictability of emerging regular auditory patterns and has been interpreted as an evidence accumulation signal. Consistent with this notion, our IDYOM analysis (Fig. 1B) finds a gradual reduction in information content for RAND10-REG10, thereby indicating expected uncertainties that may lead to a progressive model update.

(b) In REG10-RAND10, we used transitions from a regular to a random pattern. Such a transition is shown to elicit a similar response to the mismatch-negativity (MMN) in EEG (Electroencephalography) and MEG (Barascud et al., 2016; Southwell, 2019). Our IDYOM analysis (Fig. 1B) indicates an abrupt and sustained increase in information content, indicating unexpected uncertainties that may lead to a model reset.

(c) In REG10a-REG10b, we used another way of violating an already-established regularity, namely through a transition between different regular patterns (from REG10a to REG10b). Such a condition was not investigated by Zhao et al. (2019), while in the context of EEG research, it has been shown to elicit an MMN-like response (Southwell, 2019). The IDYOM analysis (Fig. 1B) showed that it evoked increased information content right after the transition, similar to what we found for REG10-RAND10. This suggests that the computational requirements required by REG10-RAND10 and REG10a-REG10b might be the same immediately after the transition. With the inclusion of this condition —which generalizes Zhao et al. (2019)— we aimed to verify that the resulting PDRs are not due to the possible saliency of a new random pattern after a regular pattern per se and instead are due to the violation of an internal model, a possible signature of a global reset signal in the brain.

Below, we show that our results confirm the results of Zhao et al. (2019). We observed PDRs to transitions that led to the violation of regularities with a remarkably similar magnitude in both the old (REG10-RAND10) and the new conditions (REG10a-REG10b) and did not observe PDRs to the emergence of regularities from random patterns (RAND10-REG10). This shows that PDRs associated with regularity violations present a robust effect. Following the interpretation of Zhao et al. (2019), we conclude that the LC-NE system, whose activation is inferred from PDRs, is sensitive to unexpected uncertainties leading to model reset but not expected uncertainties leading to model update.

2. Material and Methods

The study was preregistered at AsPredicted (https://aspredicted.org/blind.php?x=GSK_NHJ). The raw data, processed data, and analysis scripts will be shared as an Open Science Framework project upon acceptance of the manuscript.

2.1 Participants

Twenty-nine participants attended the study. As a result of the exclusion criteria based on the gap detection task specified in the preregistration, no data was collected for three participants whose accuracies after practice remained below 80%. However, due to the poor general performance of participants in finding gaps, we later deviated from the preregistration, letting all participants attend the main experiment and excluding outliers before the main analysis. Four participants with hit rates three standard deviations below or false alarm rates three standard deviations above the group mean were excluded, resulting in 22 participants (8 female, M_{age}: 24.43, SD_{age}: 3.28). Including the four excluded participants in the analysis did not change our results.

Zhao et al. (2019) reported Cohen's d_z of 0.8 in a within-subjects design with a one-sided t-test for the effect of PDRs and determined that N = 12 yields adequate power ($1 - \beta = 0.8$) at $\alpha = 0.05$. With the same effect size, we found that N = 20 increases the power to 0.964 (The current power of the study with N=22 is $1- \beta = 0.976$).

The participants were mostly university students and compensated with either course credit or 10 EUR per hour. The ethics committee of the Eberhard Karls University of Tübingen approved the study (Date of approval: 17.06.2020).

2.2 Materials

We used the same auditory stimuli as Zhao et al. (2019). All auditory stimuli were generated by concatenating 50 ms tones of various frequencies selected from a frequency pool consisting of 20 log-

spaced values between 222 and 2000 Hz (namely, 222, 250, 280, 315, 354, 397, 445, 500, 561, 630, 707, 793, 890, 1000, 1122, 1259, 1414, 1587, 1781, 2000 Hz).

Ten tones selected from the frequency pool (with replacement) were used to create regularities (REG10). Similarly, ten tones selected from the frequency pool (with replacement) were shuffled to generate random patterns (RAND10).

For trials involving a transition, ten tones were selected from the frequency pool for the first pattern, and the same tones were used to generate the second pattern to avoid introducing novel tones after the transition. There were three types of trials with transitions: (a) RAND10-REG10 involved a transition from RAND10 to REG10. These trials were used to investigate the effect of the emergence of regularity. (b) REG10-RAND10 involved a transition from REG10 to RAND10 and was used to investigate the effect of the violation of regularity. (c) REG10a-REG10b involved a transition from one REG10 pattern to another REG10 pattern and thereby also constituted a violation of a regularity (these trials generalize Zhao et al., 2019). If PDRs are sensitive to unexpected uncertainties and are evoked due to model reset, transitions in (b) and (c) should elicit PDRs but not in (a).

Each participant observed 192 randomly generated trials corresponding to 48 RAND10, 48 REG10, 48 RAND10-REG10, 24 REG10-RAND10, and 24 REG10a-REG10b. The length of the auditory sequences varied randomly between 6 and 8 s, at a granularity of 500 ms. Transitions occurred between 3 and 4 s after the sequence onset. Specifically, REG10s consisted of 12-16 repetitions of the same auditory sequence (120-160 tones in total), and REG10s in REG10-RAND10 and REG10a-REG10b were violated after 6-8 repetitions (60-80 tones in total) presented. Inter-trial intervals were 5 s.

A gap detection task was provided to keep participants' attention and lead them to engage with the auditory stimuli (Milne et al., 2021; Zhao et al., 2019). The gap detection task was orthogonal to the transitions. It required participants to detect possible gaps that could occur in 20% of trials and at any

time between 250 ms post-onset and 750 ms pre-offset. Each condition involved the same number of gaps, but their durations were determined to be three missing tones (150 ms) for RAND and two missing tones (100 ms) for REG, as in Zhao et al. (2019), to equate the difficulty of the gap detection task. Trials involving a gap or receiving a false alarm response were removed from the analysis to avoid any effect of the gap or the motor response.

The auditory stimuli were presented by headphones (Beyerdynamic DT-770 M 80 Ohm) connected to the monitor (ViewPixx/3D System, screen diagonal: 24-inch/60.96 cm). Participants were provided with a RESPONSEPixx connected to the monitor and could respond with any of the five buttons (according to their preference). The participants' right eyes were tracked using an EyeLink 1000 system (SR Research) at a 1000 Hz sampling rate.

2.3 Procedure

Participants sat in a luminance-controlled, dimly lit room (5 cd/m^2) to ensure that non-luminance-evoked pupil dilation could be observed. They were instructed to place their chin on a chinrest 50 cm away from the monitor to maintain a fixed distance between the eye and the monitor. They were asked to fixate on a white cross (13.2 cd/m^2) in the center of a grey background, which remained constant throughout the experiment. The eye tracker was positioned below the monitor and continuously tracked the gaze position and the right eye.

Sounds were presented diotically at a comfortable intensity level the participants selected before the experiment. Participants were shown several examples of auditory sequence, including a gap and a short practice session was carried out. They were instructed to monitor the sequences for silent gaps and respond by pressing a button. The end of trials was indicated by a fixation cross changing to green for 400 ms. The main experiment involved four blocks, each taking approximately 9 minutes with 3-minute optional breaks. Participants observed trials coming from different conditions within the same

block. A calibration phase was applied before each block to calibrate the gaze locations detected by the eye tracker.

2.4 Analysis

Our preprocessing pipeline closely paralleled that of Zhao et al. (2019) but was implemented using different programming languages and software packages. We note minor deviations throughout the analyses section.

2.4.1 Analysis of Gap Detection Performances

Participants' performance in the gap detection task was transformed into hit and false alarm rates. Hit and false alarm rates were then arcsine transformed for the subsequent parametric and Bayesian statistical analyses.

2.4.2 Analysis of Pupil Size Values

The area of the pupil of the right eye was measured during the experiment, and the data were converted to diameter for further analysis and comparability with Zhao et al. (2019) (pupil area led to the same results). The pupil size data were analyzed at 1000 Hz.

Participants' gaze directions were analyzed to avoid any effect of gaze on pupil size by checking deviations of more than three standard deviations from the group mean. By this criterion, we found that none of the participants' mean gaze locations exceeded the group mean by more than this amount.

As noted, trials involving a gap or receiving a false alarm response were removed from the analysis to avoid any effect of the gap or the motor response. The pupil sizes measured for RAND10-REG10, REG10-RAND10, and REG10a-REG10b conditions were separated into epochs according to the transition time; namely, the data were segmented by considering 1 second before and 3 seconds after transitions. For the conditions REG10 and RAND10, which lack a transition, dummy transition times were

randomly selected between 3 and 4 s. The segmented data were analyzed to investigate the effect of transitions on PDRs. Considering that the first ten tones in REG10 were indistinguishable from random sequences of tones, transitions from RAND10 to REG10 were shifted one repetition (10 tones, 500 ms) as in Zhao et al. (2019) for analyzing PDRs.

Complete or partial blinks in the segmented pupil size data were reconstructed by piecewise cubic interpolation. Trials having 50% missing data because of blinking or involving missing data after interpolation were removed from the analyses (≈1.15% of all trials). After blink construction, the data were smoothed with a 150 ms Hanning window.

To be able to compare the conditions, the data were z-scored by computing each participant's mean and standard deviation for each block separately across all conditions. To assess the effect of transitions on pupil size, baselines were determined for each trial as the mean of a 1-second interval before the transitions. Separate linear regressions were calculated for each participant, condition, and timepoint (each timepoint represents 1 ms) to predict the pupil dilation from the baseline, with the residuals from these regressions being used for further analysis (subtracting baselines from each trial led to similar results, see Appendix A). The data were aggregated for each participant and each condition, and were then combined based on each condition to investigate the effect of transitions on PDRs.

Finally, a series of two-tailed t-tests were conducted to compare conditions after down-sampling the data to 20 Hz. The family-wise error rate was controlled using a non-parametric permutation procedure (5000 iterations with a threshold of $p < 0.05$) by the MNE package in Python (Gramfort et al., 2013; Larson et al., 2023; Maris & Oostenveld, 2007). In contrast to the target study, the analysis was supplemented with a Bayesian analysis by transforming t values to Bayes factors (BF_{10}) with Jeffreys, Zellner, and Siow (JZS) prior using the Pingouin package in Python (Vallat, 2018). Unless stated otherwise, the transformation was conducted with a Cauchy scale factor of 0.707.

To estimate the possible baseline differences between regular and random patterns (i.e., REG10 versus RAND10), RAND10 and REG10 conditions were segmented by considering 1 second before and 6 seconds after sequence onset. Then, similar analysis steps were applied to REG10 and RAND10 separately, except for baseline correction. For baseline correction, similar to Zhao et al. (2019), the mean of the 1-second interval before the sequence onset was computed and subtracted from each trial to investigate the effect of patterns.

2.4.3 Pupil Event Rate Analysis

We estimated pupil events (i.e., pupil dilation and constriction) using the method proposed by Joshi et al. (2016) and applied by Zhao et al. (2019). The detection of events by this method focuses on either positive (i.e., pupil dilation) or negative (i.e., pupil constriction) changes in pupil size independent of the magnitude.

The slope of the change on each trial was computed by a set of linear regression algorithms trained sequentially on a 150 ms window to recover the pupil's behavior at specific time points, using time as a predictor of pupil size. The locations of pupil dilations were defined as maximum slope values; conversely, those of constrictions were defined as minimum slope values between two selected sequential zero-crossings where pupil size stays the same. Sequential zero-crossings were selected based on exceeding two different thresholds on their separation in time (Joshi et al., 2016).

Similar to Zhao et al. (2019), events were determined according to 75 and 300 ms thresholds for each trial, and event rates were computed using a 500 ms sliding window for each participant for each condition. Finally, we performed the same statistical procedure we employed for comparing PDRs to compare event rates across conditions.

3. Results

3.1 Behavioral Performance in Gap Detection Task

Participants reached similar performances on gap detection during RAND10 (with the longer gaps) and REG10 (Figure 2A). Paired two-sided t-tests over hit and false alarm rates did not reveal a significant difference (Hit rates: p=0.31, 95% CI=[-0.1, 0.3], d=0.31; False alarm rates: p=0.2, 95% CI=[-0.04, 0.01], d=0.41). Bayes factor analyses moderately favored the null hypothesis (Hit rates: BF_{10}=0.361; False alarm rates: BF_{10}=0.483). For comparison, see the results of Zhao et al. (2019) reproduced in Figure 2B. While their participants generally achieved ceiling performance, some of our participants achieved only suboptimal results.

Figure 2

Hit and false alarm rates of participants in the gap detection task

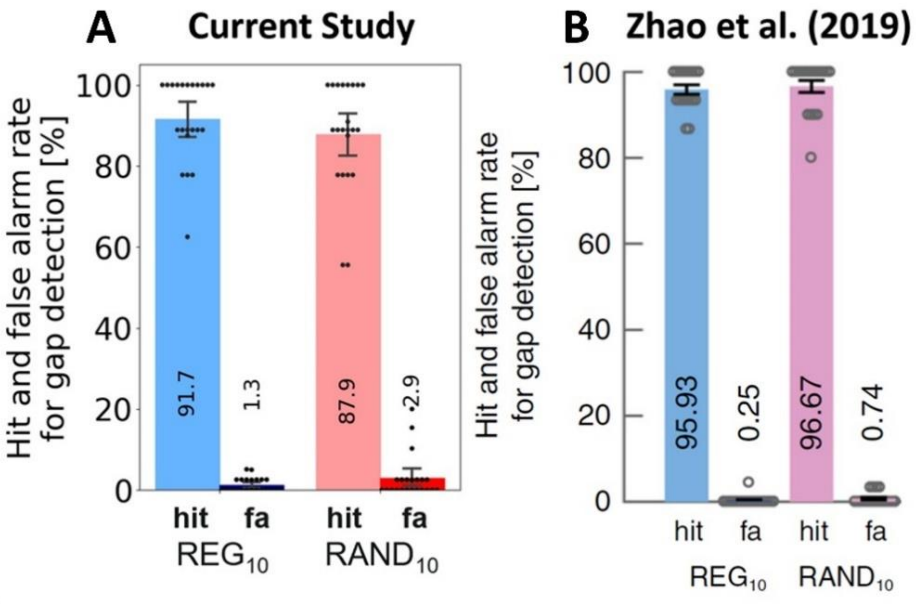

Note. (A) Gap detection performance of participants in the current study. Error bars indicate bootstrapped 95% CIs. (B) Gap detection performance in Zhao et al. (2019). Error bars indicate SEMs. The figure is adapted from Figure 5f in Zhao et al. (2019) and has been modified to exclude the irrelevant condition RAND20 under the Creative Commons Attribution 4.0 International License (CC BY 4.0).

3.2 Analysis of PDRs

The emergence of auditory regularities in RAND10-REG10 trials did not induce PDRs. By contrast, the violation of auditory regularities in REG10-RAND10 trials did elicit PDRs (Figure 3A). This result agrees with the results of Zhao et al. (2019) regarding the shape and magnitude of PDRs (reproduced in Figure 3B). Confirming the results of Zhao et al. (2019), we observed that the pupil responds to regularity violations at around 620 ms. Specifically, BF_{10}>1 is observed at 620 ms (BF_{10}=1.10) and BF_{10}>3 at 700 ms (BF_{10}=4.17). After that, the pupil diameter increases steeply until 1500 ms, with a normalized magnitude of approximately 0.2, gradually dropping. Bayesian and frequentist statistical tests suggested that pupil size for REG10-RAND10 was still higher than baseline at the end of the epoch (BF_{10}=2.59 and p=0.051).

Similarly, REG10a-REG10b, the violation of auditory regularities and the emergence of new regularities, elicited PDRs (Figure 3C). Similar to REG10-RAND10, PDRs in REG10a-REG10b deviated from REG10, the baseline, at approximately 560 ms. Specifically, BF_{10} value exceeds 1 at 560 ms (BF_{10}=1.03) and 3 at 660 ms (BF_{10}=3.43). The results of statistical tests suggest that pupil response times to REG10a-REG10b might be earlier than those to REG10-RAND10.

Both Bayesian and frequentist statistical tests indicate that the evidence for differing pupil sizes gradually decreases for REG10a-REG10b. This trend is observable at 2750 ms (REG10a-REG10b: BF_{10}=1.63, *p*=0.09; REG10-RAND10: BF_{10}=2.23, p=0.062) and continues at 3000 ms (REG10a-REG10b: BF_{10}=0.95, *p*=0.20; REG10-RAND10: BF_{10}=2.59, p=0.051). However, the direct comparison between the two conditions was not statistically significant (mean statistical values 2-3 s post-transition: BF_{10}=0.26, *p*=0.52, d_z=0.18).

Figure 3

The violation of regularities elicits PDRs

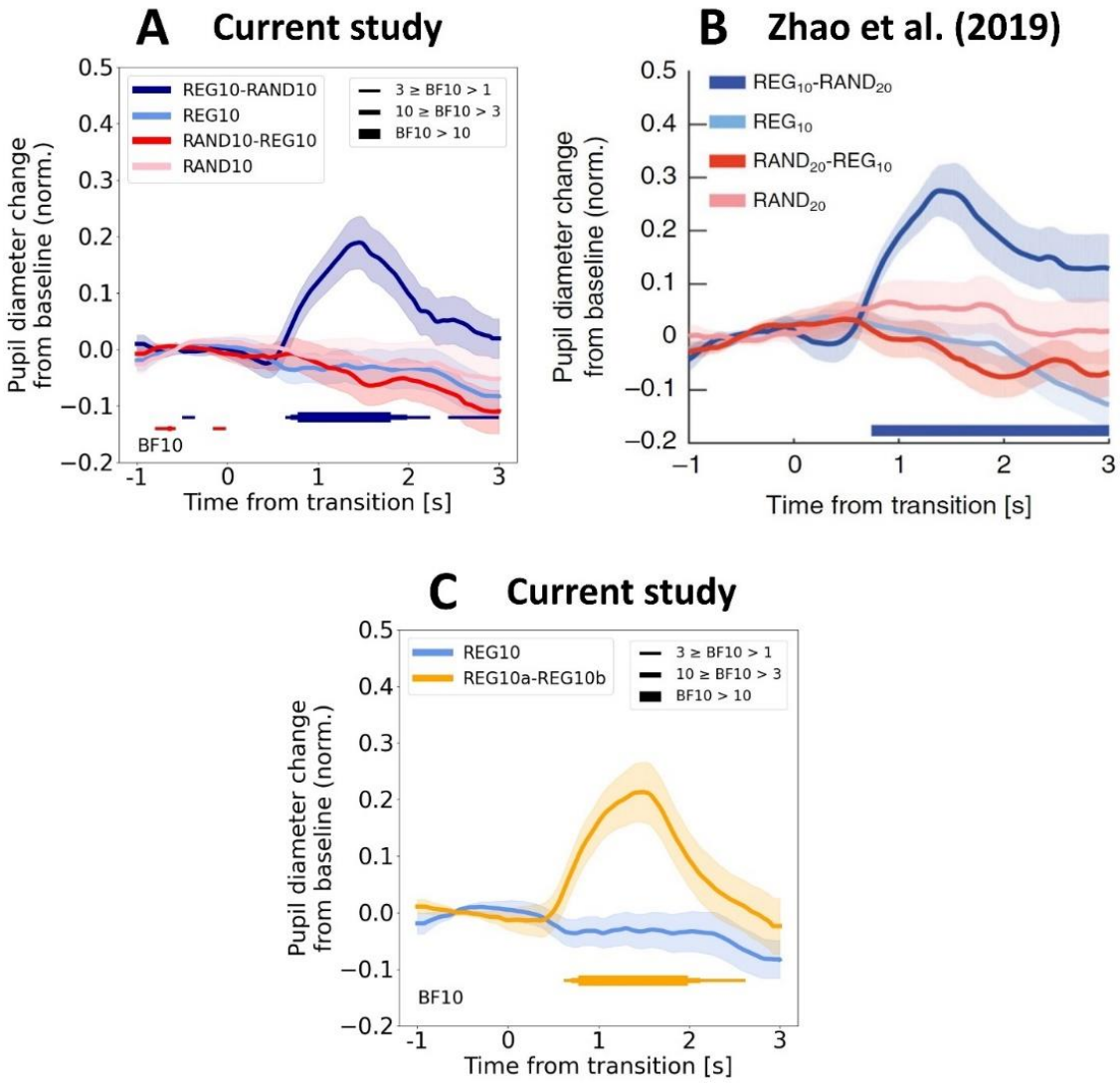

Note. Pupil size as a function of time in (A) our study, as well as in (B) Zhao et al. (2019). Comparing (A) and (B) shows the strong resemblance of the results: PDRs were induced by the violation of regular patterns (REG10-RAND10) but not by the emergence of regular patterns (RAND10-REG10). Also, pupil size for REG10-RAND10 was still higher than baseline at the end of the epoch. (C) Pupil size for our study's new REG10a-REG10b condition. Like REG10-RAND10, a violation of regularities evoked PDRs. Note that pupil sizes for REG10a-REG10b were close to baseline at the end of the epoch (cf. main text). Figure (B) corresponds to Figure 5a of Zhao et al. (2019). Note that the random patterns shown in this figure are based on 20 tones (RAND20). We used this figure because all relevant conditions can be seen in this figure, and Zhao et al. (2019) found no qualitative difference in PDRs between random patterns generated by 10 and 20 tones. Colored horizontal lines indicate statistics for the difference between each transition condition and the no-transition control condition: In (A) and (C), those statistics correspond to the Bayes factors BF_{10} > 1, 3, and 10 (represented by varying thickness levels), and in (B) they correspond to p<0.05 in the two-tailed t-tests as described in Section 2.4.2. Shaded areas indicate the between-participant SEMs. This figure was reprinted from Figure 5a of Zhao et al. (2019) according to the Creative Commons Attribution 4.0 International (CC BY 4.0 DEED).

3.3 Analysis of Sustained Pupil Sizes

To examine whether pattern type affects sustained pupil sizes, we compared pupil sizes in REG10 and RAND10. Figure 4A shows no considerable difference between REG10 and RAND10, suggesting that PDRs to the violation of regularities (REG10-RAND10 and REG10a-REG10b) but not to the emergence of regularities (RAND10-REG10) are not a side effect of baseline pupil size differences between RAND10 and REG10.

This finding is consistent with the results of Zhao et al. (2019) (reproduced in Figure 4B). Regarding the dynamics of pupil response to the sequence onset, both studies observed a sharp increase in pupil size by the first 1.5 s. Our results reveal a plateau in pupil size at around 0.45 for both conditions, less than the pupil size amplitude observed in the target study. In our study, pupil responses to sound onset seem slower but slightly steeper.

Figure 4

Sustained pupil responses to regular and random patterns

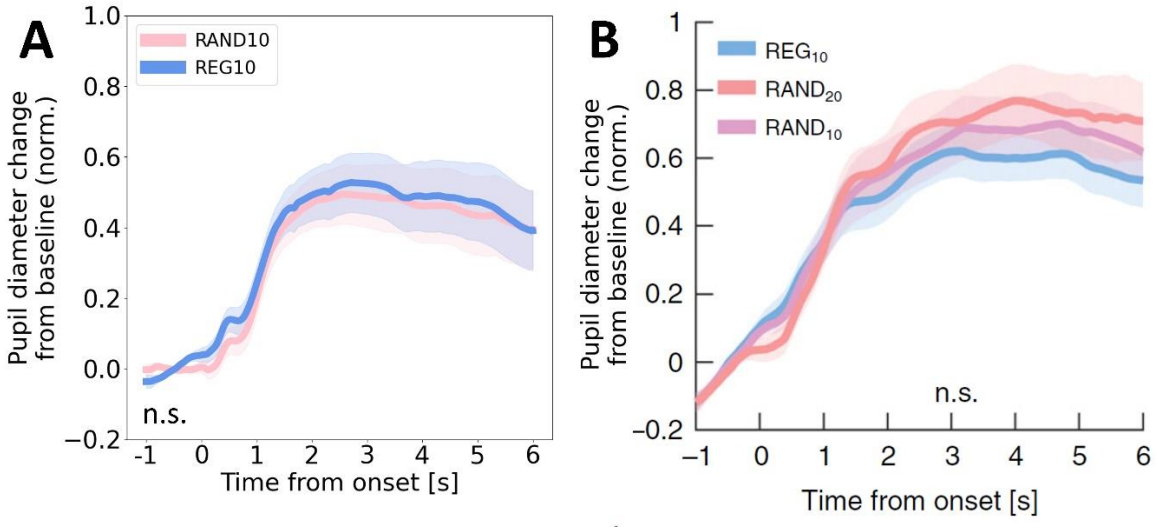

Note. Average normalized pupil size over time in baseline conditions. (A) shows pupil diameter changes from our study, and (B) shows those of Zhao et al. (2019). Similar to Zhao et al. (2019), we did not observe a difference between baseline conditions. The shaded area indicates the between-participant SEM. (B) represents Figure 5e, reprinted from Zhao et al. (2019) according to the Creative Commons Attribution 4.0 International (CC BY 4.0 DEED).

3.4 Pupil Event Rate Analysis

Pupil event rate analysis conducted using 75 and 300 ms thresholds for the minimum gaps between successive detections yielded comparable patterns with Zhao et al. (2019). Note that our study includes 22 participants, whereas the results from Zhao et al. (2019) include 32 participants from two experiments.

Figure 5A shows that dilation rates for REG10-RAND10 and REG10a-REG10b became apparent after the transition at around 500 ms (Figure 5B reanalyzed from Zhao et al., 2019 for pupil dilation rates). The transition from RAND10 to REG10 did not lead to an increase in pupil dilation rate.

Figures 5A and 5C show that pupil constriction rates mirrored dilation rates, such that constriction rates started to decrease at around 500 ms, and the minimum constriction rate was observed at about 750 ms in REG10-RAND10 and REG10a-REG10b. Constriction rates after transitions observed in REG10-RAND10 and REG10a-REG10b revealed the possibility of an orienting response (Strauch et al., 2022; see our Figure 5C), which is not strong in the data of Zhao et al. (Figure 5D reanalyzed from Zhao et al., 2019 for pupil constriction rates). On the other hand, there was a slight increase, rather than a decrease, in the constriction rates in RAND10-REG10 after the transition.

Although we observed similar pupil dilation and constriction patterns to those of Zhao et al. (2019), our results diverged from the reported baseline event rates. After reanalyzing their publicly available data, we determined that the event rates should be approximately 0.75 Hz and 0.35 Hz for 75 ms and 300 ms, respectively, and not 3 Hz and 1.4 Hz, as Zhao et al. (2019) reported. S. Zhao confirmed these revised estimates (S. Zhao, personal communication, June 12, 2023). With these revised estimates, our findings align closely with those of Zhao et al. (2019) (compare Figures 5A and 5B with Figures 5C and 5D).

Figure 5

Pupil event rate analyses

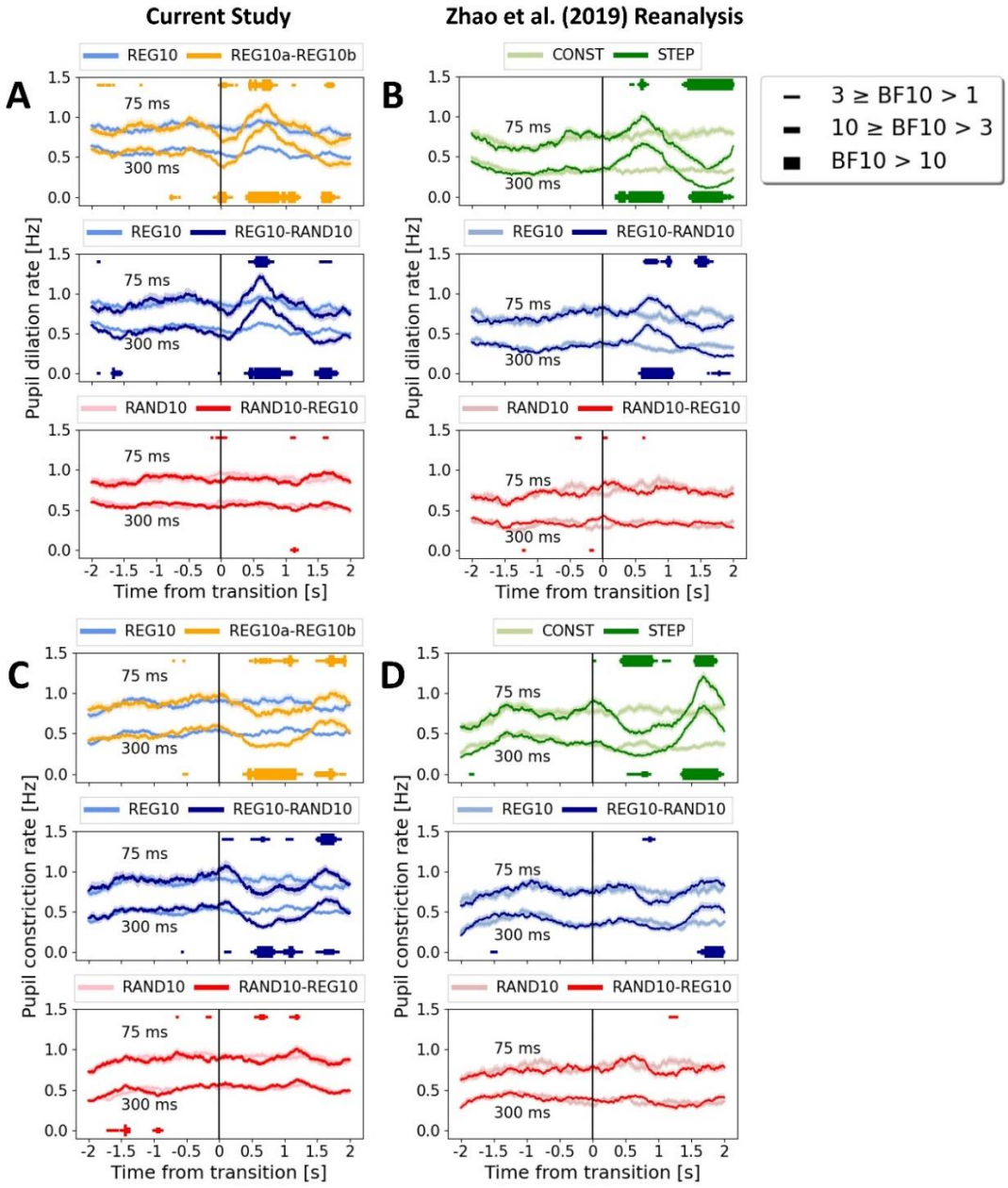

Note. Pupil dilation rates (A, B) and pupil constriction rates (C, D) were computed using a running average with a 500 ms window. Figures A and C were derived from the data collected in this study. In contrast, Figures B and D show the data provided by Zhao et al. (2019) and reanalyzed by us (see the main text). With these revised estimates, our findings align closely with those of Zhao et al. (2019) regarding both pupil event rate patterns and baseline event rates. Colored horizontal lines indicate regions where cluster-level statistics show BF_{10} > 1, 3, and 10 (represented by varying thickness levels) between each transition condition and the no-transition control. These lines are positioned above and below the graphs corresponding to the 75 ms and 300 ms thresholds, respectively. Shaded areas represent the between-participant SEMs.

3.4 Further Analyses

We used linear regression-based baseline correction for comparability with Zhao et al. (2019). As an exploratory analysis, we reanalyzed data with a classical baseline correction method, namely subtractive baseline correction, where pupil baselines were subtracted trial-by-trial (Appendix A). The type of baseline correction did not change the main pattern of PDRs (Figure 3) but resulted in slightly higher magnitudes and overlapping pupil response times (BF_{10}>1 at 620 ms and BF_{10}>3 at 680 ms for both REG10-RAND10 and REG10a-REG10b). To pinpoint when pupils respond to regularity violations, we conducted an exploratory analysis based on pupil dilation events (Appendix B for details). Most evidence suggests that pupils, on average, respond to regularity violations between 600 and 650 ms.

We also observed that most participants showed an increase in pupil size in response to regularity violations. Namely, in a group of 22 participants, 18 from REG10a-REG10b and 17 from REG10-RAND10 exhibited a pupil size increase after the transition, albeit with a high variability (Appendix C). Additionally, a strong and reliable correlation existed between REG10-RAND10 and REG10a-REG10b (r=0.62, BF_{10}=21.81, 95% *CI*=[0.27, 0.82]).

In each trial, REG10a and REG10b were randomly selected from REG10a-REG10b, resulting in patterns with varying degrees of difference that could influence the properties of PDRs (Appendix D). As part of an exploratory analysis, we quantified the dissimilarity between REG10a and REG10b using edit distance methods commonly employed in computational linguistics and natural language processing literature (Wagner & Fischer, 1974; Navarro, 2001; Yu et al., 2016). We observed using linear-mixed effect models that the distances between REG10a and REG10b could positively influence magnitudes of PDRs ($\beta \approx 0.05$, $R^2 \approx 0.37$) but had little or no impact on their temporal properties.

4. Discussion

We replicated and generalized the results of Zhao et al. (2019) on how changes in patterns of fast-paced tone pips are associated with pupil dilation and constriction. Similar to Zhao et al. (2019), auditory sequences involved transitions from RAND10 to REG10 patterns and from REG10 to RAND10 patterns. We confirmed that the emergence of regularities from random patterns did not lead to PDRs. In contrast, the violation of regularities by random patterns evoked PDRs with notable similarities in shape and magnitude to Zhao et al. (2019).

We generalized Zhao et al. (2019) using a novel, but conceptually similar, condition to induce regularity violations (REG10a-REG10b). We showed that transitions between two regular patterns also evoked PDRs, supporting the idea that it is not the presence of random patterns but the violation of the antecedent regularity that leads to PDRs. Therefore, we can conclude that abrupt model violation, but not progressive model update, leads to PDRs.

Moreover, we observed a constriction response after PDRs evoked by the REG10a-REG10b condition, with the average pupil size reaching the level of REG10 at 3 s after the transition. On the other hand, in the REG10-RAND10 condition, the average pupil size showed a slight and gradual constriction response but did not return to its baseline. However, a direct comparison of the two conditions did not reveal strong evidence of a difference (cf. Section 3.2 and Appendix A). We suggest further research investigating the relationship between pupil response profiles and learning.

Statistical tests and exploratory analyses suggest that although participants' pupil response times varied, pupils responded to regularity violations -on average- after 600 ms. This aligns with the results of Joshi et al. (2016), demonstrating that the LC electrical microstimulation leads to maximum evoked pupil size change after approximately 500 ms in primates. Considering that the human brain

needs around 150 ms to detect violation of these regularities (Barascud et al., 2016), we consider that the detected pupil reaction times align well with the literature.

We observed that distances between REG10a and REG10b positively affected PDRs' magnitudes but had little or no effect on their temporal dynamics. This result suggests that although these metrics capture some aspects of participants' perceptual changes, they fail to explain their temporal evolution. This limitation is understandable, as these metrics do not account for the timing of changes and are indifferent to the location in the sequences where the differences occur. Our exploratory results suggest that the relationship between perceptual similarity judgments, distance methods, and PDRs to regularity violations merits further investigation (Wagner & Fischer, 1974; Tversky, 1977; Navarro, 2001; Yu et al., 2016; Zhao et al., 2019).

Despite the consistent findings of PDRs in response to regularity violations, we observed individual and intra-individual differences in our analyses. Many factors affect PDRs associated with regularity violations. Those may include, but are certainly not limited to, participants' performance in the irrelevant task, baseline pupil sizes before a transition, similarities between sound sequences before and after a transition, and changes in information content. In our analyses, we could not offer strong suggestions regarding the relationships between these factors and properties of PDRs; further research should investigate how PDRs to regularity violations evolve with these factors.

Overall, these results suggest that PDRs are a reliable biomarker of the violation of an already established internal model. In this respect, they have a resemblance with the MMN, a specific negative neural response shown in EEG and MEG to deviant events that violate a simple, sequential standard tone or abstract rule-based structures (Paavilainen, 2013). Further research inspired by the MMN literature should investigate the conditions that can modulate PDRs associated with model reset. Furthermore, future studies should investigate PDRs associated with the reset of models built for

different modalities, such as vision or tactile, or the properties of models built in conjunction with other models. Through this approach, the relationship between different types of internal models and their relationships with the arousal system can be better understood.

5. Conclusion

Many studies suggest that phasic LC-NE activation relates to PDRs (de Gee et al., 2017; Joshi & Gold, 2020; Murphy et al., 2014; Reimer et al., 2016); thereby, the PDR is considered a biomarker of the NE and arousal response in the cortices. Our results directly supported the conclusion of Zhao et al. (2019) that PDRs are associated with internal model reset as a response to unexpected environmental changes. PDRs seem to reveal the sensitivity of the LC-NE system to unexpected uncertainty even when it is not behaviorally relevant, consistent with its role as a form of neural reset signal.

6. Appendices

A. Subtractive Baseline Correction

In the main text, we described a baseline correction procedure based on a linear regression. We did this to ensure comparability with Zhao et al. (2019). Additionally, and for completeness, we here describe an alternative analysis using subtractive baseline correction. This method extracts baseline effects by subtracting the mean of the 1-second interval before a transition from the rest of the trial, aligning the average baseline pupil size values to zero for all trials. We will show that the results of both baseline correction methods are mostly similar.

Similar to the baseline correction with linear regression, the emergence of auditory regularities did not induce PDRs, and the violation of auditory regularities elicited PDRs (Figure A.1). There was a slight difference, though, because the onsets of the PDRs now overlap, which was not the case when using the linear regression-based baseline correction. Specifically, for $BF_{10}>1$ (REG10-RAND10: $BF_{10}=1.32$ at 620 ms; REG10a-REG10b: $BF_{10}=1.25$ at 620 ms) and for $BF_{10}>3$ (REG10-RAND10: $BF_{10}=3.58$ at 680 ms;

REG10a-REG10b: BF_{10}=3.24 at 680 ms). After a sharp response, the pupil shows a steep increase until 1500 ms, with a magnitude over 0.2, after which it gradually drops.

Figure A.1

PDRs with subtractive baseline correction.

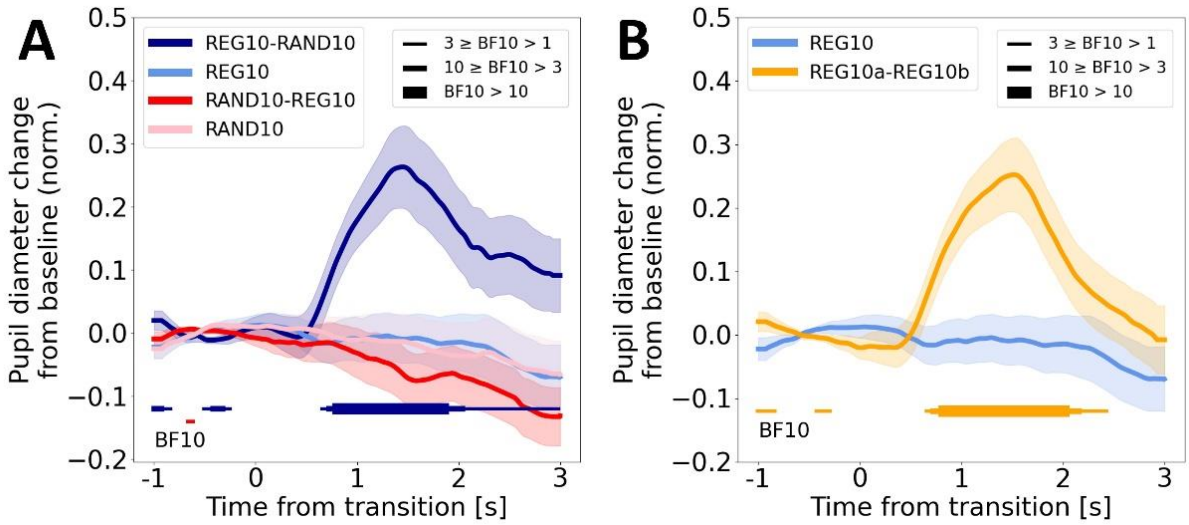

Note. Average normalized pupil size over time relative to the transition. (A) Pupil size for REG10-RAND10 was still higher than the baseline at the end of the epoch. (B) Pupil diameter changes for REG10a-REG10b from our study. Similar to REG10-RAND10, the violation of regularities evoked PDRs. The pupil size for REG10a-REG10b turned to its baseline at the end of the epoch (cf. main text). Colored horizontal lines indicate regions where cluster-level statistics show BF10 > 1, 3, and 10 (represented by varying thickness levels) to indicate the difference between each transition condition and the no-transition control. Shaded areas indicate the between-participant SEMs.

Both Bayesian and frequentist statistical tests indicate that the evidence for differing pupil sizes gradually decreases for REG10a-REG10b (Figure A.1A) but not for REG10a-RAND10 (Figure A.1B). This trend is visible at 2750 ms (REG10a-REG10b: BF_{10}=1.30, p=0.128; REG10-RAND10: BF_{10}=3.74, p=0.032) and continues by the end of the trial (REG10a-REG10b: BF_{10}=0.83, p=0.247; REG10-RAND10: BF_{10}=3.58, p=0.034). Even though subtractive baseline correction emphasizes the possible difference between conditions more than linear regression-based baseline correction, the direct comparison again did not show a statistically significant effect (mean statistical values 2-3 s post-transition: BF_{10}=0.43, p=0.22, d_z=0.35).

In our exploratory analyses (except Appendix B, which is based on pupil event rate analysis), we used data from subtractive baseline correction. This method adjusts all trials' average baseline pupil size values to zero, enabling inter-individual and intra-individual analyses. Moreover, it resulted in similar pupil response profiles between the two regularity violation conditions regarding response times and magnitudes, allowing a less biased comparison.

B. Analysis of Pupil Response Times

In order to find out when pupils responded to violations of regularities, we used positive slopes computed for event rate analysis. We identified the timing of the first positive slope following a zero crossing after a transition as the response time of the pupil. We considered both thresholds, 75 ms and 300 ms, resulting in two sets of pupil response times (see Section 2.4.3).

Pupil response times estimated according to a 75 ms threshold suggest that the pupil responds approximately 600 ms after the transition (REG10-RAND10: M=602 ms, SEM=31; REG10a-REG10b: M=615, SEM=34). The response according to a 300 ms threshold agrees with this result but with an approximately 50 ms extra delay (REG10-RAND10: M=675, SEM=34; REG10a-REG10b: M=645, SEM=30). These numbers agree with Bayesian statistical tests and pupil event rate analyses. Thus, we can conclude that pupils, on average, respond to regularity violations between 600 and 650 ms.

C. Analysis of Mean Pupil Responses

We wanted to understand whether all participants showed a response to violations of regularities. To assess this, we determined mean pupil responses (estimated by subtractive baseline correction) for each trial by averaging the changes in pupil diameter during the 600-3000 ms interval following a transition, a time frame where mean PDRs were visible (Figure A.1) and $BF_{10}>1$ for both REG10-RAND10, REG10a-REG10b.

We observed that most participants' pupil size increased following transitions, violating regularities. Specifically, out of 22 participants, 18 in the REG10a-REG10b and 17 in the REG10-RAND10 demonstrated a pupil size increase after the transition (Figure C.1A). Indeed, pupil sizes following two types of regularity violations showed a high and reliable correlation (r=0.62, BF_{10}=21.81, 95% *CI*=[0.27, 0.82], Figure C.1B), which suggests that a similar underlying mechanism is at play. Conversely, although the emergence of regularities predominantly led to a reduction in pupil size (N=16), the degree of decrease was less than the increase in pupil size observed in response to regularity violations.

Figure C.1

Individual variabilities in mean pupil responses

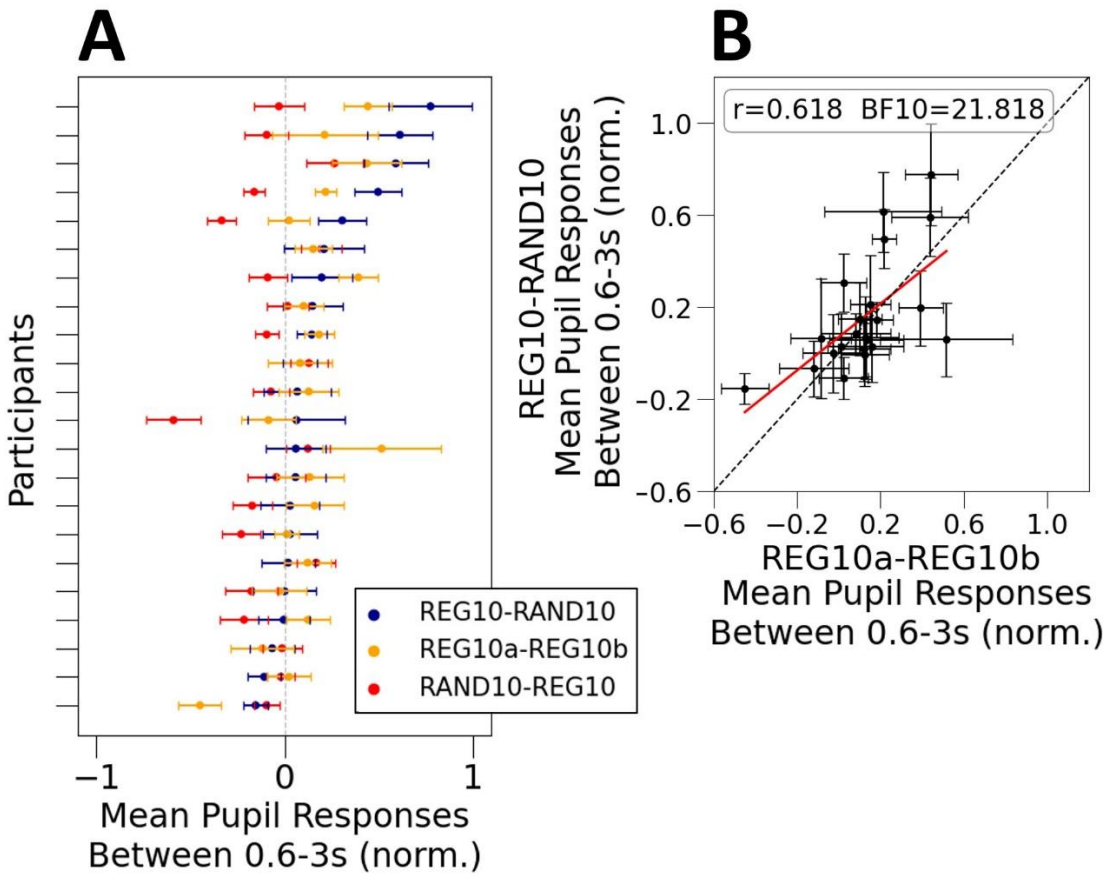

Note. (A) represents the mean pupil responses of participants, averaged over the time range of 0.6-3 s and sorted according to values shown for REG10-RAND10. (B) shows the correlation between mean pupil responses to regularity violations. Error bars represent SEMs.

D. Distance Analyses

We randomly sampled regularities in REG10a-REG10b for each trial. Therefore, the difference between regularities before (REG10a) and after the transition (REG10b) may affect PDRs. In order to explore this effect, we estimated differences between regularities by conventional edit distance methods (distance methods for short). We related them to PDRs by linear mixed-effect models implemented with the lme4 package in R.

Commonly used in computational linguistics and natural language processing, distance methods employ character-based operations—namely, insertion, deletion, substitution, and transposition—to quantify the dissimilarity between two strings (Wagner & Fischer, 1974; Navarro, 2001; Yu et al., 2016). Insertion adds (e.g., 'ab' -> 'cab'), deletion removes (e.g., 'ab' -> 'a'), substitution alters (e.g., 'ab' -> 'ac'), and transposition swaps (e.g., 'ab' -> 'ba') a character. We used the following methods from the strsimpy and Levenshtein modules in Python to cover possible operations:

- Hamming Distance: This method quantifies the dissimilarity between two strings by counting the minimum **substitutions** needed to turn one string into another.
- Circular Hamming Distance: This method quantifies the similarity between two strings, considering the minimum number of **substitutions** after all possible circular shifts.
- Jaro Distance: Besides **substitutions**, this method considers **transpositions** between subsequent characters.
- Longest Common Subsequence: A subsequence in a string follows a left-to-right order but does not require consecutive characters. The longest common subsequence is a measure that finds the longest sequence shared between two strings with the minimum number of **insertions** and **deletions**. If the length of the shared subsequence is long, the two strings are less distant.

- Levenshtein Distance: This method considers the fewest **insertions, deletions, and substitutions** needed to convert one string to another.
- Damerau-Levenshtein Distance: As an extension of the Levenshtein distance, this method considers **insertion, deletion, substitution, and transposition** operations.

Correlations of distance methods for REG10a-REG10b trials varied considerably between 0.21 (Hamming vs. Circular Hamming Distances) and 0.97 (Levenshtein and Damerau-Levenshtein Distances). Circular Hamming Distance exhibited a low correlation with other methods, standing almost isolated (Figure D.1A). Given the strong correlation between methods, we also computed Principal Component Analysis (PCA) to extract a main principal component, which explained 0.848 of the total variances.

We applied min-max normalization to distance values, including the principal component, to be able to compare computed coefficients. This technique scales features in a dataset to a standard range, namely [0, 1], by subtracting the minimum value from each feature and dividing it by the range.

Along with mean pupil responses and pupil response times (Appendix B and C), we computed two additional variables: peak pupil responses and peak pupil response times. Next, we excluded outlier observations that deviated more than three standard deviations from the mean to ensure the data reflected typical trends. We calculated participants' sensitivities (d') from hit and false alarm rates and used them along with pupil baselines as nuisance variables in linear-mixed models. These models had varying intercepts for each participant. Adding varying slopes was unfeasible due to the limited size of the data and the risk of overfitting.

Firstly, we investigated the relationship between distance values and PDR magnitudes, namely mean and peak pupil responses. The model predicting mean pupil responses yielded a good fit ($R^2 \approx 0.24$). However, none of the coefficients was statistically significant ($\beta \approx 0.04$). The model predicting peak pupil responses yielded a better fit ($R^2 \approx 0.37$, $\beta \approx 0.05$), suggesting that distances between two

regularities were associated with slightly larger PDRs. Most coefficients, including the principal component, were in the predicted direction (Figure D.1B, error bars represent 95% *CI, t* values were computed using the Satterthwaite method).

On the other hand, we observed that models predicting pupil response and peak times yielded poor fits ($R^2 \approx 0.02$). This result implies that the distances between regularities, in conjunction with sensitivities and baseline pupil size, may not reliably predict the timing of pupil dynamics.

Figure D.1

Distance analyses

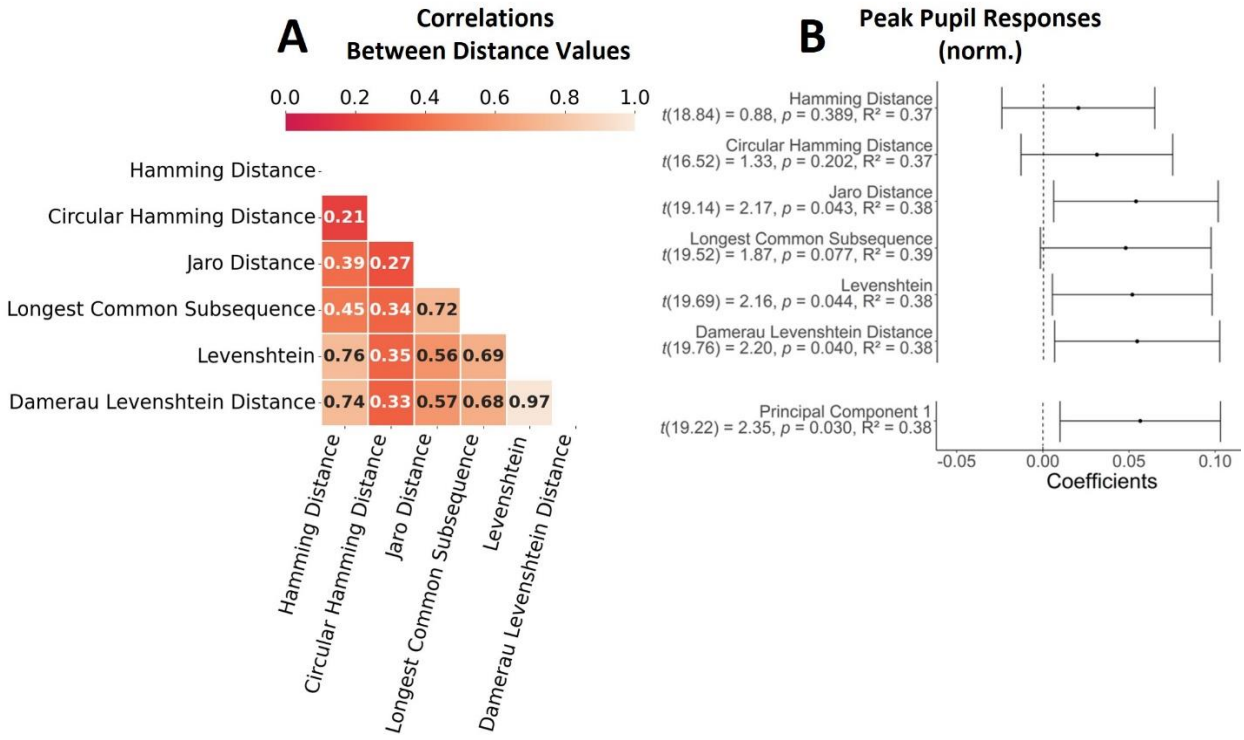

Note. (A) Pearson correlations between distances estimated for REG10a-REG10b. Correlation coefficients range from 0.21 to 0.97. (B) Coefficients for distances and their principal component as predictors of peak pupil responses. Error bars denote 95% CIs.

7. Acknowledgements

The study was supported by the German Research Foundation (DFG, SFB 1233 "Robust Vision", TP 05, No 276693517), the Max Planck Society and Humboldt Foundation (Peter Dayan), and Machine Learning Cluster of Excellence, EXC 2064/1 No 390727645 (Volker Franz). We are most grateful to Dr. Sijia Zhao for sharing data and code and for her generous and speedy responses to queries. Portions of these findings were presented as posters at the ECVP 2022, TeaP 2022, and Psychonomics 2023.

References

Aston-Jones, G., & Cohen, J. D. (2005). An integrative theory of locus coeruleus-norepinephrine function: Adaptive gain and optimal performance. *Annual Review of Neuroscience*, *28*(1), 403–450. https://doi.org/10.1146/annurev.neuro.28.061604.135709

Barascud, N., Pearce, M. T., Griffiths, T. D., Friston, K. J., & Chait, M. (2016). Brain responses in humans reveal ideal observer-like sensitivity to complex acoustic patterns. *Proceedings of the National Academy of Sciences*, *113*(5). https://doi.org/10.1073/pnas.1508523113

Bestmann, S., Harrison, L. M., Blankenburg, F., Mars, R. B., Haggard, P., Friston, K. J., & Rothwell, J. C. (2008). Influence of uncertainty and surprise on human corticospinal excitability during preparation for action. *Current Biology*, *18*(10), 775–780. https://doi.org/10.1016/j.cub.2008.04.051

Bouret, S., & Sara, S. J. (2005). Network reset: a simplified overarching theory of locus coeruleus noradrenaline function. *Trends in Neurosciences*, *28*(11), 574-582.

Canale, R. The importance of statistical learning. *Nature Reviews Psychology* 1, 68 (2022). https://doi.org/10.1038/s44159-021-00010-2

Carter, M. E., Yizhar, O., Chikahisa, S., Nguyen, H., Adamantidis, A., Nishino, S., Deisseroth, K., & de Lecea, L. (2010). Tuning arousal with optogenetic modulation of locus coeruleus neurons. *Nature Neuroscience*, *13*(12), 1526–1533. https://doi.org/10.1038/nn.2682

Dayan, P., & Yu, A. J. (2003). Uncertainty and learning. *IETE Journal of Research*, *49*(2–3), 171–181. https://doi.org/10.1080/03772063.2003.11416335

Dayan, P., & Yu, A. J. (2006). Phasic norepinephrine: A neural interrupt signal for unexpected events. *Network: Computation in Neural Systems*, *17*(4), 335–350. https://doi.org/10.1080/09548980601004024

de Gee, J. W., Colizoli, O., Kloosterman, N. A., Knapen, T., Nieuwenhuis, S., & Donner, T. H. (2017). Dynamic modulation of decision biases by brainstem arousal systems. *ELife*, *6*, e23232. https://doi.org/10.7554/eLife.23232

Farashahi, S., Donahue, C. H., Khorsand, P., Seo, H., Lee, D., & Soltani, A. (2017). Metaplasticity as a neural substrate for adaptive learning and choice under uncertainty. *Neuron*, *94*(2), 401-414.e6. https://doi.org/10.1016/j.neuron.2017.03.044

Frost, R., Armstrong, B. C., & Christiansen, M. H. (2019). Statistical learning research: A critical review and possible new directions. *Psychological Bulletin, 145*(12), 1128–1153. https://doi.org/10.1037/bul0000210

Gershman, S. J., & Niv, Y. (2010). Learning latent structure: carving nature at its joints. *Current Opinion in Neurobiology*, *20*(2), 251-256. https://doi.org/10.1016/j.conb.2010.02.008

Joshi, S., & Gold, J. I. (2020). Pupil size as a window on neural substrates of cognition. *Trends in Cognitive Sciences*, *24*(6), 466–480. https://doi.org/10.1016/j.tics.2020.03.005

Joshi, S., Li, Y., Kalwani, R. M., & Gold, J. I. (2016). Relationships between pupil diameter and neuronal activity in the locus coeruleus, colliculi, and cingulate cortex. *Neuron*, *89*(1), 221–234. https://doi.org/10.1016/j.neuron.2015.11.028

Krishnamurthy, K., Nassar, M. R., Sarode, S., & Gold, J. I. (2017). Arousal-related adjustments of perceptual biases optimize perception in dynamic environments. *Nature Human Behaviour*, *1*(6), 0107. https://doi.org/10.1038/s41562-017-0107

Marshall, L., Mathys, C., Ruge, D., de Berker, A. O., Dayan, P., Stephan, K. E., & Bestmann, S. (2016). Pharmacological fingerprints of contextual uncertainty. *PLOS Biology*, *14*(11), e1002575. https://doi.org/10.1371/journal.pbio.1002575

Milne, A. E., Zhao, S., Tampakaki, C., Bury, G., & Chait, M. (2021). Sustained pupil responses are modulated by predictability of auditory sequences. *The Journal of Neuroscience*, *41*(28), 6116–6127. https://doi.org/10.1523/JNEUROSCI.2879-20.2021

Murphy, P. R., O'Connell, R. G., O'Sullivan, M., Robertson, I. H., & Balsters, J. H. (2014). Pupil diameter covaries with BOLD activity in human locus coeruleus. *Human Brain Mapping*, *35*(8), 4140–4154. https://doi.org/10.1002/hbm.22466

Navarro, G. (2001). A guided tour to approximate string matching. ACM computing surveys (CSUR), 33(1), 31-88.

Nassar, M. R., Rumsey, K. M., Wilson, R. C., Parikh, K., Heasly, B., & Gold, J. I. (2012). Rational regulation of learning dynamics by pupil-linked arousal systems. *Nature Neuroscience*, *15*(7), 1040–1046. https://doi.org/10.1038/nn.3130

Paavilainen, P. (2013). The mismatch-negativity (MMN) component of the auditory event-related potential to violations of abstract regularities: A review. *International Journal of Psychophysiology*, *88*(2), 109–123. https://doi.org/10.1016/j.ijpsycho.2013.03.015

Payzan-LeNestour, E., Dunne, S., Bossaerts, P., & O'Doherty, J. P. (2013). The neural representation of unexpected uncertainty during value-based decision making. *Neuron*, *79*(1), 191–201. https://doi.org/10.1016/j.neuron.2013.04.037

Reimer, J., McGinley, M. J., Liu, Y., Rodenkirch, C., Wang, Q., McCormick, D. A., & Tolias, A. S. (2016). Pupil fluctuations track rapid changes in adrenergic and cholinergic activity in cortex. *Nature Communications*, *7*(1), 13289. https://doi.org/10.1038/ncomms13289

Sara, S. J., & Bouret, S. (2012). Orienting and reorienting: The locus coeruleus mediates cognition through arousal. *Neuron*, *76*(1), 130–141. https://doi.org/10.1016/j.neuron.2012.09.011

Soltani, A., & Izquierdo, A. (2019). Adaptive learning under expected and unexpected uncertainty. *Nature Reviews Neuroscience*, *20*(10), 635–644. https://doi.org/10.1038/s41583-019-0180-y

Strauch, C., Wang, C.-A., Einhäuser, W., Van der Stigchel, S., & Naber, M. (2022). Pupillometry as an integrated readout of distinct attentional networks. *Trends in Neurosciences*, *45*(8), 635–647. https://doi.org/10.1016/j.tins.2022.05.003

Tversky, A. (1977). Features of similarity. *Psychological Review*, *84*(4), 327.

Vallat, R. (2018). Pingouin: Statistics in Python. *Journal of Open Source Software*, *3*(31), 1026. https://doi.org/10.21105/joss.01026

Wilson, R. C., Nassar, M. R., & Gold, J. I. (2013). A mixture of delta-rules approximation to Bayesian inference in change-point problems. *PLoS Computational Biology*, *9*(7), e1003150.

Wagner, R. A., & Fischer, M. J. (1974). The string-to-string correction problem. *Journal of the ACM (JACM)*, *21*(1), 168-173.

Yu, A. J., & Dayan, P. (2005). Uncertainty, neuromodulation, and attention. *Neuron*, *46*(4), 681–692. https://doi.org/10.1016/j.neuron.2005.04.026

Yu, M., Li, G., Deng, D., & Feng, J. (2016). String similarity search and join: a survey. *Frontiers of Computer Science*, 10, 399-417.

Zhao, S., Chait, M., Dick, F., Dayan, P., Furukawa, S., & Liao, H.-I. (2019). Pupil-linked phasic arousal evoked by violation but not emergence of regularity within rapid sound sequences. *Nature Communications*, *10*(1), 4030. https://doi.org/10.1038/s41467-019-12048-1